Ferrata Storti Foundation

# Human BCR/ABL1 induces chronic myeloid leukemia-like disease in zebrafish

**Mengchang Xu,[1] Yin Ye,[2] Zhi'an Ye,[1] Song'en Xu,[1] Wei Liu,[2] Jin Xu,[2] Yiyue Zhang,[2] Qifa Liu,[3] Zhibin Huang,[2] and Wenqing Zhang[1,2]**

[1]Key Laboratory of Zebrafish Modeling and Drug Screening for Human Diseases of Guangdong Higher Education Institutes, Department of Developmental Biology, School of Basic Medical Sciences, Southern Medical University; [2]Division of Cell, Developmental and Integrative Biology, School of Medicine, South China University of Technology and [3]Department of Hematology, Nanfang Hospital, Southern Medical University, Guangzhou, China

**Haematologica** 2020
Volume 105(3):674-686

## ABSTRACT

Chronic myeloid leukemia (CML) is induced by the *BCR/ABL1* oncogene, which encodes a protein tyrosine kinase. We examined the effect of direct overexpression of the human $p210^{BCR/ABL1}$ oncoprotein in zebrafish. Humanized $p210^{BCR/ABL1}$ protein was detectable in *Tg(hsp70:*$p210^{BCR/ABL1}$*)* transgenic zebrafish embryos and adult kidney marrow. Transgenic zebrafish developed CML, which could be induced *via* cells transplanted into recipients. The expression of human *BCR/ABL1* promoted myeloid lineages in *Tg(hsp70:*$p210^{BCR/ABL1}$*)* transgenic embryos. A total of 77 of 101 (76.24%) *Tg(hsp70:*$p210^{BCR/ABL1}$*)* adult transgenic zebrafish (age 6 months-1 year) developed CML. CML in zebrafish showed a triphasic phenotype, similar to that in humans, involving a chronic phase predominantly characterized by neutrophils in various degrees of maturation, an accelerated phase with an increase in blasts and immature myeloid elements, and a blast phase with >90% blasts in both the peripheral blood and kidney marrow. Tyrosine kinase inhibitors, as the standard drug treatment for human CML, effectively reduced the expanded myeloid population in *Tg(hsp70:*$p210^{BCR/ABL1}$*)* transgenic embryos. Moreover, we screened a library of 171 compounds and identified ten new drugs against BCR/ABL1 kinase-dependent or -independent pathways that could also reduce *lcp1*$^{+}$ myeloid cell numbers in *Tg(hsp70:*$p210^{BCR/ABL1}$*)* transgenic embryos. In summary, we generated the first humanized zebrafish CML model that recapitulates many characteristics of human CML. This novel *in vivo* model will help to elucidate the mechanisms of CML disease progression and allow high-throughput drug screening of possible treatments for this disease.

## Introduction

Chronic myeloid leukemia (CML) is a malignant bone marrow proliferative tumor originating from hematopoietic stem cells (HSC), with an annual incidence of 1-2/100,000 and accounting for 15-20% of all adult leukemias.[1] CML is characterized by uncontrolled proliferation of myeloid cells and their progenitors in the peripheral blood (PB) and bone marrow (BM).[2] The development of CML progresses from a chronic phase (CP) to an accelerated phase (AP), and finally to a blast phase (BP). Most patients in the CML-CP are clinically asymptomatic, but are diagnosed with leukocytosis characterized by mature granulocytes in the PB and BM. Disease progression to AP and BP is accompanied by a severe reduction in cellular differentiation, with immature blasts displacing mature cells.[3] The final transformation phase can result in both lymphoblastic (25%) and myeloblastic (50%) subtypes, with a further 25% manifesting biphenotypic or undifferentiated phenotypes.[4]

The presence of the Philadelphia chromosome ($Ph^{+}$) is an important diagnostic indicator for CML.[5] It is generated by a reciprocal translocation between chromosomes 9 and 22, referred to as t(9;22)(q34;q11).[6] This translocation results in the *BCR/ABL1* fusion gene, which is translated to the $p210^{BCR/ABL1}$ oncoprotein in almost

**Correspondence:**

*WENQING ZHANG*
mczhangwq@scut.edu.cn

*ZHIBIN HUANG*
huangzhb1986@scut.edu.cn

Received: January 4, 2019.

Accepted: July 5, 2019.

Pre-published: July 9, 2019.

doi:10.3324/haematol.2019.215939

*Check the online version for the most updated information on this article, online supplements, and information on authorship & disclosures: www.haematologica.org/content/105/3/674*

all patients with CML.[7,8] This fusion protein is a constitutively active tyrosine kinase that persistently activates various signaling pathways regulating cell proliferation, transformation, and survival, thereby promoting leukemogenesis.[9] Further research and exploration are needed to recognize the blast crisis of CML since the specific mechanism leading to it is not yet fully understood.

The therapeutic use of tyrosine kinase inhibitors (TKI), such as imatinib, dasatinib, and bosutinib, has transformed the management of CML, largely turning a lethal disorder into a chronic condition. However, conventional TKI therapy for CML still presents challenges, including the appearance of TKI-resistant BCR/ABL1 mutants[10] and the relative resistance of CML leukemia stem cells (LSC)[11] to TKI. In addition, all TKI have a similar spectrum of toxic effects[4] that can negatively affect the patient's quality of life. Furthermore, CML and other malignancies include a population of cancer stem cells (CSC) that is able to regenerate or self-renew, resulting in therapeutic resistance and disease progression, and the inability to eradicate these CSC remains a significant obstacle to curing these diseases.

Biomedical research requires suitable animal disease models in which to study the mechanisms responsible for the cellular and molecular pathologies, and for testing certain therapeutic methods. There are high levels of conservation in terms of genomics, histoembryology, physiology, cardiac electrophysiology, and drug metabolic pathways between zebrafish and humans,[12] and zebrafish thus represent a possible model for studying hematopoietic development and for high-throughput drug screening. However, there is currently no zebrafish CML model. The construction of a zebrafish CML model would expand our ability to study this disease and to develop new drugs that could benefit CML patients.

## Methods

### Zebrafish husbandry

All experiments involving zebrafish were carried out in accordance with the guidelines set by the Institutional Animal Care and Use Committee of Southern Medical University, Guangzhou, China. Zebrafish were raised, bred, and staged according to standard protocols.[13,14] The following strains were used: AB (wild-type strain, WT) and *Tg(lyz:DsRed)*.[15]

### Generation of the pToL *hsp70*:p210$^{BCR/ABL1}$ construct and of *Tg(hsp70:p210*$^{BCR/ABL1}$*)* transgenic zebrafish

The transgenic construct consisted of the zebrafish heat shock protein (Hsp) 70 promoter, human *BCR/ABL1* (h*BCR/ABL1*) (b3a2) cDNA, Tol2 elements, and the SV40 polyA sequence. We cloned *hsp70* promoter elements by polymerase chain reaction (PCR) using *hsp70*-specific primers 5′-GTATCGATTCAGGGGTGTCGCTTGGT-3′ and 5′-CCGATATCACCGGTCTGCAGGAAAAAAAAAC-3′. The h*BCR/ABL1* (b3a2) cDNA fragment was isolated from the plasmid NGFR P210[16] (Addgene) after digestion with EcoRI. The *hsp70* promoter sequence was then placed upstream of the h*BCR/ABL1* (b3a2) cDNA and subcloned into the pToL vector with minimal Tol2 elements and an SV40 polyA sequence to form the pToL *hsp70*:p210$^{BCR/ABL1}$ construct. The transgenic line was generated by injecting 50 pg of the pToL *hsp70*:p210$^{BCR/ABL1}$ construct together with Tol2 transposase mRNA into zebrafish embryos at the one-cell stage. Founders were identified by PCR confirmation of the transgene.

### Western blot

Protein was extracted from whole embryos at 6 days post-fertilization (dpf) or from blood cells from the kidney marrow (KM) of 1-year-old *Tg(hsp70:p210*$^{BCR/ABL1)}$ and age-matched WT controls. Proteins were quantified, and assessed by western blot analysis. Protein lysates were probed with rabbit anti-c-Abl antibody (1:1000 dilution, Cell Signaling Technology). Mouse anti-glyceraldehyde 3-phosphate dehydrogenase (GAPDH) antibody (1:5000 dilution, Cell Signaling Technology) was included as an internal control.

### Cell proliferation assay

Wild-type (WT) and *Tg(hsp70:p210*$^{BCR/ABL1)}$ embryos at 3 dpf and 1-year old adults were incubated in 10 mM BrdU (Sigma-Aldrich) for 2 hours (h) and 4 h, respectively. The embryos and KM blood cells were stained with mouse-anti-BrdU antibody (Roche) and rabbit-anti-Lcp1 antibody (gift from Dr. Zilong Wen),[17] followed by Alexa Fluor 555-anti-mouse antibody (Invitrogen) and Alexa Fluor 488-anti-rabbit antibody (Invitrogen) for fluorescent visualization.

### Terminal deoxynucleotidyl transferase dUTP nick end labeling assay

Transferase dUTP nick end labeling (TUNEL) assay was carried out using an *In Situ* Cell Death Detection Kit (TMR red, Roche), followed by rabbit anti-Lcp1 antibody and Alexa Fluor 488-anti-rabbit antibody (Invitrogen) for fluorescent visualization.

### Transplantation

Whole KM cell suspensions were prepared from *Tg(lyz:DsRed)* and *Tg(hsp70:p210*$^{BCR/ABL1}$*-lyz:DsRed*) (CML-like) fish. Three days after receiving a sublethal dose of radiation (25 Gy), 0.2 million cells were injected intracardially into irradiated WT recipients using a glass capillary needle (World Precision Instruments).

### Drug treatment

Embryos were soaked in egg water containing 1‰ dimethylsulfoxide (DMSO) (Sigma-Aldrich), 20 μmol/L imatinib (Selleck), 5 μmol/L dasatinib (Selleck), 10 μmol/L bosutinib (Selleck), 20 μmol/L LY364947 (MedChemExpress), 2.5 μmol/L FTY720 (MedChemExpress), 0.5 μmol/L BEZ235 (MedChemExpress), or compounds from a compound library (TargetMol) for drug treatment.

### Statistical analysis

Data were analyzed using SPSS software (version 20). Differences between two groups were analyzed using Student *t*-tests and differences among multiple groups by one-way analysis of variance (ANOVA) with Tukey's adjustment. Significance was accepted when $P<0.05$. Data were expressed as mean±Standard Error of Mean (SEM).

Details of other methods used are available in the *Online Supplementary Appendix*.

## Results

### Transient expression of humanized BCR/ABL1 increased the number of myeloid cells in zebrafish larvae

The *BCR/ABL1* fusion gene is present in nearly all cases of CML. Protein sequence comparisons revealed that zebrafish Bcr and Abl1 shared around 71% and 73% identities, respectively, with their human counterparts and contained a highly conserved kinase domain on Abl1

(Ensembl GRCh37 release 92). We evaluated the function of the hBCR/ABL1 oncoprotein in zebrafish by overexpressing h*BCR/ABL1* mRNA encoding the $p210^{BCR/ABL1}$ oncoprotein. We then detected the numbers of myeloid cells during embryonic hematopoietic development by *lcp1, lyz, mpx* whole-mount *in situ* hybridization (WISH), and Sudan Black B (SB) cytochemical staining (Figure 1). *lcp1*, also named *l-plastin*, is a pan-myeloid marker that identifies all myeloid subsets, including macrophages and neutrophils. Numbers of *lcp1*$^+$ cells were significantly

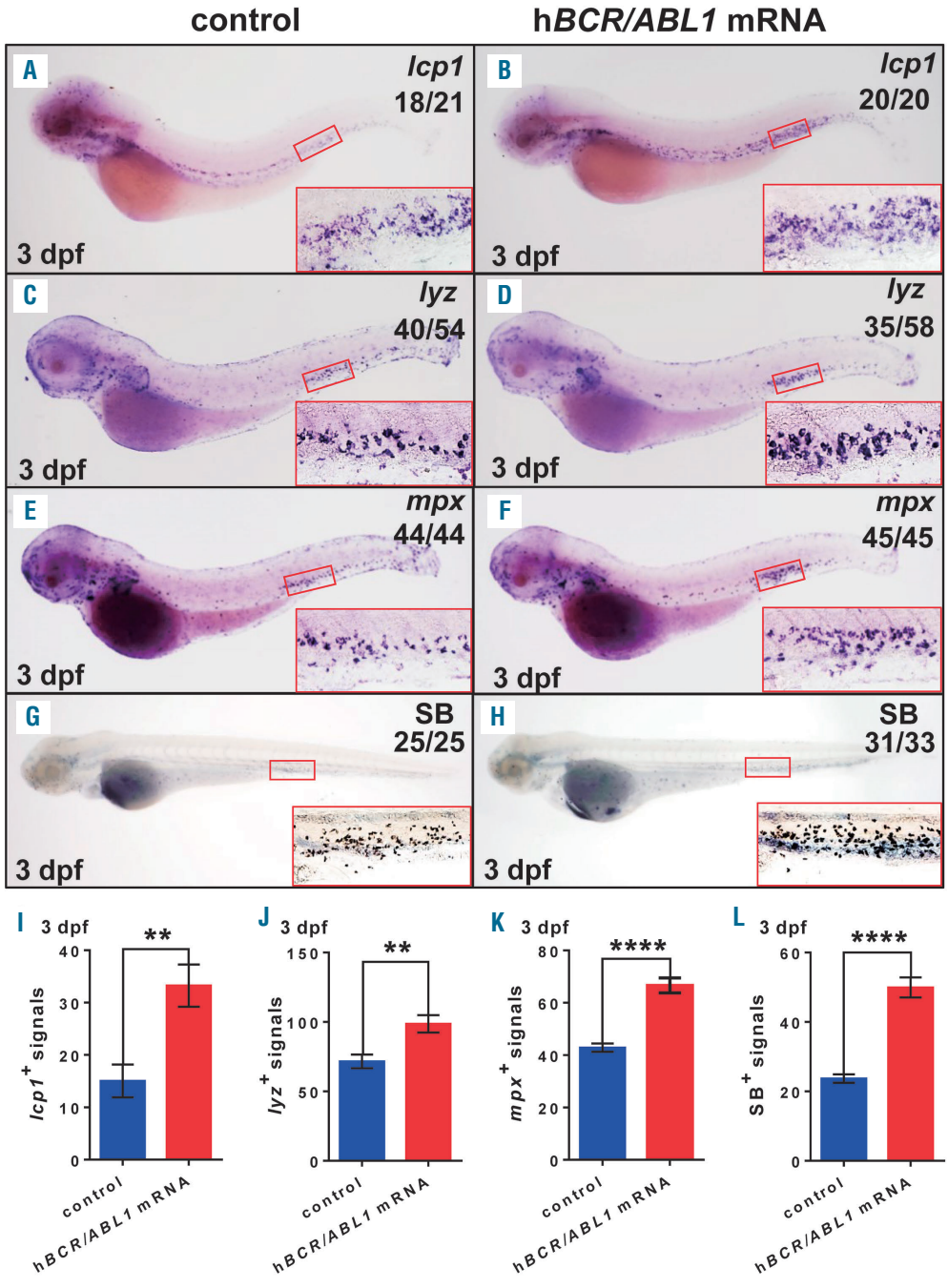


**Figure 1. Expression levels of myeloid markers (*lcp1, lyz, mpx* and SB) increased after transient expression of humanized *BCR/ABL1* (h*BCR/ABL1*) in zebrafish larvae.** Whole mount *in situ* hybridization (WISH) of *lcp1* (A and B), *lyz* (C and D), and *mpx* (E and F) expressions in wild-type (WT) zebrafish larvae after transient overexpression of h*BCR/ABL1* mRNA (right) were higher than controls (left) at 3 dpf. (G and H) The number of SB$^+$ cells in WT zebrafish larvae after transient overexpression of h*BCR/ABL1* mRNA (right) was higher than controls (left) at 3 dpf. n/n: number of zebrafish larvae showing representative phenotype/total number of zebrafish larvae examined. Original magnification ×32 (A-H). Red rectangles in each panel indicate the signals in PBI region, and the regions were enlarged at the lower right (original magnification ×200). (I-L) Statistical analysis. *lcp1*$^+$ signals (I), *lyz*$^+$ signals (J), *mpx*$^+$ signals (K), and SB$^+$ signals (L) in PBI region after injection were calculated and compared at 3 dpf (Student *t*-tests, mean±Standard Error of Mean, $^{**}P<0.01$; $^{****}P<0.0001$).

increased after overexpression of hBCR/ABL1 compared with the control group. Expression levels of markers of more mature neutrophils, such as *lyz, mpx,* and SB, also increased significantly. Patients with CML typically develop a highly characteristic differential white blood cell (WBC) count with high concentrations of myelocytes and segmented neutrophils. The current results implied that hBCR/ABL1 expression in zebrafish may promote myelocytes and may be capable of inducing myeloid leukemia *in vivo*.

### *hBCR/ABL1* was inherited in *Tg(hsp70:p210$^{BCR/ABL1}$)* transgenic zebrafish

*Tg(hsp70:p210$^{BCR/ABL1}$)* transgenic zebrafish were created using a construct (Figure 2A) expressing h*BCR/ABL1 under* the control of the zebrafish heat shock-inducible *hsp70* promoter.[18,19] The construct was designed to integrate the complete coding sequence into the host genome using the Tol2 transposition system, allowing the generation of multiple lines of transgenic zebrafish. *Tg(hsp70:p210$^{BCR/ABL1}$)* transgenic zebrafish founders were confirmed by PCR (Figure 2B). Stable F1 *Tg(hsp70:p210$^{BCR/ABL1}$)* transgenic zebrafish were obtained by intercrossing founder fish and were confirmed by sequencing (*data not shown*). F2 and the offsprings were obtained by mating F1 fish with WT fish. The temporospatial expression of h*BCR/ABL1* in *Tg(hsp70:p210$^{BCR/ABL1}$)* transgenic zebrafish was evaluated by WISH (Figure 2C). h*BCR/ABL1* expression was apparent throughout the body of *Tg(hsp70:p210$^{BCR/ABL1}$)* embryos at 3 dpf after heat shock treatment. Further detection by real-time-quantitative (RT-q)-PCR showed that levels of h*BCR/ABL1* mRNA were significantly elevated after heat shock treatment in both *coro1a*:GFP$^{+}$ blood cells from *Tg(hsp70:p210$^{BCR/ABL1}$)* transgenic zebrafish embryos and hematopoietic progenitors and myelocytes in KM blood cells from *Tg(hsp70:p210$^{BCR/ABL1}$)* transgenic zebrafish adults (*Online Supplementary Figure S1*). The h*BCR/ABL1* oncogene encoding the p210$^{BCR/ABL1}$ protein was also detected in *Tg(hsp70:p210$^{BCR/ABL1}$)* transgenic zebrafish embryos and adult kidneys (Figure 2D). The molecular weight of p210$^{BCR/ABL1}$ measured *in vitro* (*Online Supplementary Figure S2*) confirmed that the weight of the fusion protein generated was as expected. The p210$^{BCR/ABL1}$ protein was highly expressed in *Tg(hsp70:p210$^{BCR/ABL1}$)* transgenic zebrafish after heat-shock treatment.

### Inducible h*BCR/ABL1* expression in *Tg(hsp70:p210$^{BCR/ABL1}$)* transgenic zebrafish promoted myeloid lineage in zebrafish embryos

Expression of p210$^{BCR/ABL1}$ induces leukemia and myeloproliferative disorders, indicating a direct, causal role of BCR/ABL in CML.[9,20-23] We established *Tg(hsp70:p210$^{BCR/ABL1}$)* transgenic zebrafish with expression of p210$^{BCR/ABL1}$ and stable inheritance. To further explore the function of p210$^{BCR/ABL1}$ in zebrafish, we observed its influence on hematopoietic development in zebrafish embryos using WISH and cytochemical staining with lineage-specific markers (Figure 2E). The numbers of *lcp1*$^{+}$ pan-myeloid cells, *lyz*$^{+}$ neutrophils, SB$^{+}$ neutrophils, and *mfap4*$^{+}$ macrophages were significantly increased in *Tg(hsp70:p210$^{BCR/ABL1}$)* transgenic zebrafish larvae at 3 dpf compared with WT controls. This suggested that h*BCR/ABL1* expressed in zebrafish could either promote the production of HSC or their differentiation into each hematopoietic lineage. To distinguish between these possibilities, we detected the HSC marker (*cmyb*), erythrocyte marker (*βe1*), and lymphocyte marker (*rag1*). There was no difference in the number of *cmyb*$^{+}$ HSCs between *Tg(hsp70:p210$^{BCR/ABL1}$)* transgenic zebrafish and WT controls at 36 hpf, but the number was significantly increased in transgenic zebrafish at 60 hpf (*Online Supplementary Figure S3A-D, I and J*). Numbers of *βe1*$^{+}$ erythrocytes and *rag1*$^{+}$ lymphocytes were significantly decreased in the transgenic zebrafish compared with the WT control zebrafish at 5 dpf (*Online Supplementary Figure S3E-H*). These findings suggest that hBCR/ABL1 may promote myeloid differentiation.

### Inducible hBCR/ABL1 expression in *Tg(hsp70:p210$^{BCR/ABL1}$)* adult zebrafish created phenotype resembling human CML

The natural progression of untreated CML is bi- or triphasic, with the initial CP followed by AP, BP, or both. CP is characterized by leukocytosis in both the PB and BM, and a preponderance of granulocytes in various degrees of maturation. However, blasts account for <2% of the peripheral WBC and <5% of the nucleated cells in the BM.[24] As the disease progresses, patients enter the AP followed by the BP, during which there is hematopoietic differentiation arrest, allowing immature blasts to accumulate in the BM and spill into the circulation. A level of 10-19% of blasts in the PB or BM marks the transition from CP to AP, along with a predominance of promyelocytes. A level of at least 20% PB or BM blasts indicates the progression to the BP.[24] To explore the possibility of developing leukemia-like hematologic disorders in *Tg(hsp70:p210$^{BCR/ABL1}$)* adult fish, PB and KM cells were collected from *Tg(hsp70:p210$^{BCR/ABL1}$)* and WT fish at 6 months to 1-year old and subjected to cytological and WBC analyses (Table 1 and Figure 3A and B). Seventy-seven of 101 (76.24%) *Tg(hsp70:p210$^{BCR/ABL1}$)* adult zebrafish developed CML-like disease, including 68 with a CML-CP phenotype, marked by massive leukocytosis in the PB or KM, including increased percentages of myelocytes and myeloid precursors. In the early stage of CML-CP, the increased leukocytes were primarily neutrophils in various degrees of maturation. Myelocytes accounted for >15% in the PB or >50% in the KM, with blasts usually accounting for <2% of the PB and <5% of the KM during this phase. We referred to this period as CML-CP1 (Table 2). Differentiation was then interrupted in the late stage of CML-CP as the condition progressed towards CML-AP. The increased leukocytes were primarily myeloid precursors and blasts, with myeloid precursors >10% and blasts >2% in the PB, and myeloid precursors >15% and blasts >5% in the KM. We referred to this period as CML-CP2 (Table 2). Eight of the 77 CML-like *Tg(hsp70:p210$^{BCR/ABL1}$)* transgenic zebrafish showed CML-AP phenotype including significant 2- to 10-fold increases in the percentages of blasts and myeloid precursors, with blasts >10% in the PB or KM. Amongst the 77 CML-like *Tg(hsp70:p210$^{BCR/ABL1}$)* adult zebrafish, one progressed to CML-BP with >90% blasts expanding in both the PB and KM. We also identified some phenotypes accompanying these CML-like *Tg(hsp70:p210$^{BCR/ABL1}$)* adult zebrafish, including eosinophilia, lymphocytosis and thrombocytosis (Figure 3C). Six of 77 (7.79%) CML-like *Tg(hsp70:p210$^{BCR/ABL1}$)* adult zebrafish presented with eosinophilia, with eosinophils accounting for >0.1% of

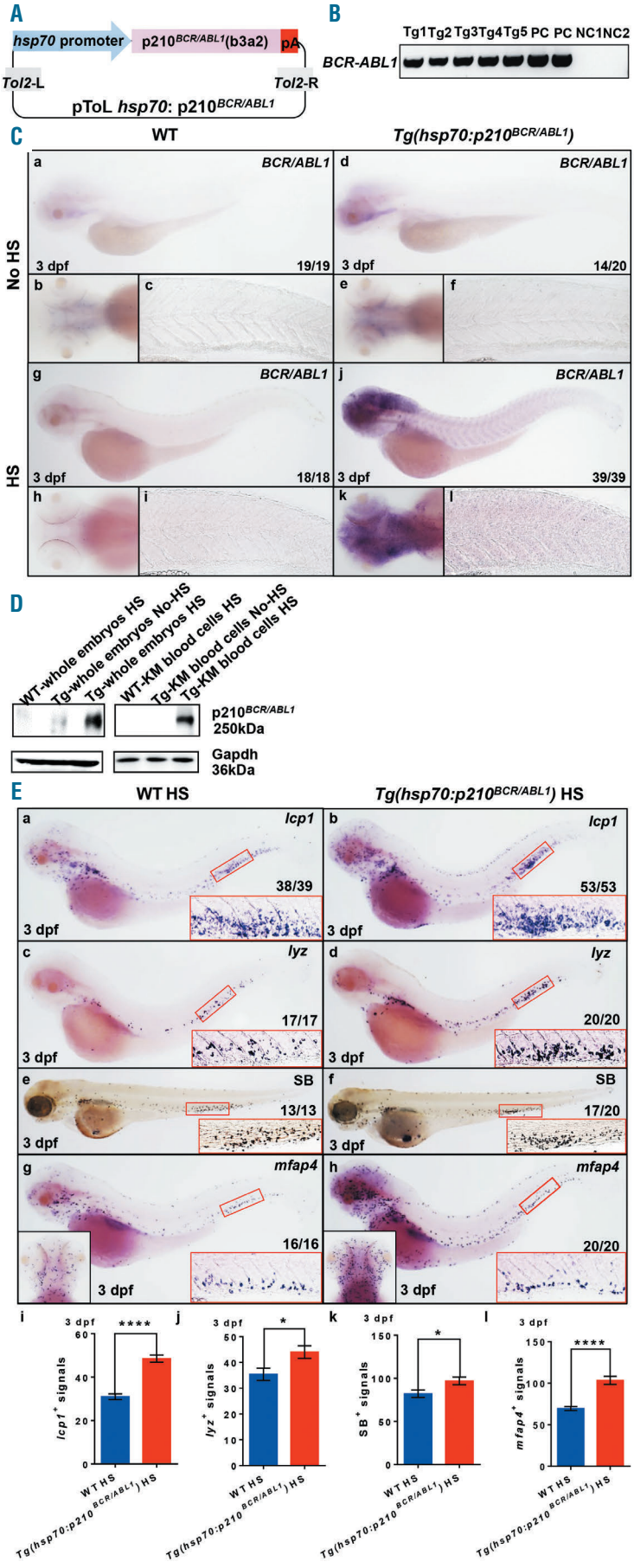


**Figure 2. Expression of h*BCR/ABL1* in *Tg(hsp70:p210$^{BCR/ABL1}$)* transgenic zebrafish.** (A) Structure of pToL *hsp70*:p210$^{BCR/ABL1}$. (B) Detection of the hBCR/ABL1 cDNA sequence integrated into the wild-type (WT) zebrafish genome using the specific polymerase chain reaction (PCR) amplifying a 466 bp fragment within the h*BCR/ABL1* fusion section. Tg: *Tg(hsp70:p210$^{BCR/ABL1}$)* founder individuals; PC: pToL *hsp70*:p210$^{BCR/ABL1}$ plasmid as the positive control; NC1: dd$H_2O$ as the negative control; NC2: genomic DNA of WT fish as the negative control. (C) Whole mount *in situ* hybridization (WISH) of h*BCR/ABL1* mRNA temporospatial expression in 3 dpf WT and *Tg(hsp70:p210$^{BCR/ABL1}$)* zebrafish embryos without (a-f) or with (g-l) heat-shock treatment. Original magnification x32 (a, d, g and j). Signals in head (b, e, h, k) and tail (c, f, i, l) region under 100× and 200× magnification, respectively. n/n: number of zebrafish embryos showing representative phenotype/total number of zebrafish embryos examined. (D) Expression of p210$^{BCR/ABL1}$ expressed in embryos (n=200) and kidney marrow (KM) blood cells (approx. $2x10^6$ cells) of *Tg(hsp70:p210$^{BCR/ABL1}$)* adult zebrafish assessed by western blot. GAPDH as the loading control. Tg: *Tg(hsp70:p210$^{BCR/ABL1}$)* transgenic zebrafish; No-HS: T*Tg(hsp70:p210$^{BCR/ABL1}$)* transgenic zebrafish without heat-shock treatment; HS: *Tg(hsp70:p210$^{BCR/ABL1}$)* transgenic zebrafish with heat-shock treatment. (E) WISH of *lcp1* (a-b), *lyz* (c-d), and *mfap4* (g-h) expressions in HS *Tg(hsp70:p210$^{BCR/ABL1}$)* (right) were higher than WT controls (left) at 3 dpf. (e-f) The number of SB positive cells in HS *Tg(hsp70:p210$^{BCR/ABL1}$)* (right) was higher than WT controls (left) at 3 dpf. n/n: number of zebrafish larvae showing representative phenotype/total number of zebrafish larvae examined. Original magnification ×32 (a-h). Red rectangles in each panel indicate the signals in PBI region and the regions were enlarged at the lower right (original magnification ×200). Black rectangles in the panel indicate the signals in the brain region (vertical view, original magnification ×50). (i-l) Statistical analysis. *lcp1*$^+$ signals (i), *lyz*$^+$ signals (j), *mfap4*$^+$ signals (l), and SB$^+$ signals (k) in PBI region were calculated and compared at 3 dpf. Student *t*-tests, mean±Standard Error of Mean; *$P$<0.05; ****$P$<0.0001.

the PB cell count compared with approximately 0.01±0.00% in WT adult zebrafish (n=55) (*Online Supplementary Table S1*). This was similar to the "Ph-positive eosinophilic/basophilic CML" described by Goh *et al.*[24] Large numbers of lymphocytes accumulated in the PB in 8 of 77 (10.39%) CML-like *Tg(hsp70:p210$^{BCR/ABL1}$)* adult zebrafish, accounting for >5% of the PB cell count compared with around 1.80±0.23% in WT adult zebrafish (n=55) (*Online Supplementary Table S1*), similar to the lymphocytosis[25] observed in CML patients. Thrombocytosis[26] is present in approximately half of all newly diagnosed CML patients. Thirteen of the 77 (16.88%) CML-like *Tg(hsp70:p210$^{BCR/ABL1}$)* adult zebrafish presented with thrombocytosis, with platelets accounting for >0.5% of the PB cell count compared with around 0.11±0.04% in WT adult zebrafish (n=55) (*Online Supplementary Table S1*). Histological examination of the spleen in CML-like *Tg(hsp70:p210$^{BCR/ABL1}$)* demonstrated expansion of the splenic red pulp, predominantly by granulocytic myeloid cells (Figure 3D). In addition, the morbidity of CML-like disease in heat-shock-treated *Tg(hsp70:p210$^{BCR/ABL1}$)* adult zebrafish was higher than in non-induced *Tg(hsp70:p210$^{BCR/ABL1}$)* adult zebrafish. The ratios of individuals in CML-CP2 and CML-AP were increased among heat-shock-treated *Tg(hsp70:p210$^{BCR/ABL1}$)* compared with untreated *Tg(hsp70:p210$^{BCR/ABL1}$)* adult zebrafish (Figure 3E). This result suggests that overexpression of BCR/ABL1 is an important factor in accelerating the course of CML.

### *Tg(hsp70:p210$^{BCR/ABL1}$)* transgenic fish displayed abnormal myeloid cell expansion resulting from increased proliferation and inhibition of apoptosis

The above results indicated that myeloid cells accumulated in *Tg(hsp70:p210$^{BCR/ABL1}$)* fish from the embryonic stage to the adult, which could be caused by accelerated proliferation or reduced apoptosis. To clarify the cellular mechanisms responsible for myeloid cell expansion in *Tg(hsp70:p210$^{BCR/ABL1}$)* fish, we monitored myeloid cell proliferation and death by BrdU incorporation and TUNEL assay, respectively. BrdU incorporation was significantly increased in *Tg(hsp70:p210$^{BCR/ABL1}$)* larvae and adult KM compared with WT controls, indicating that myeloid cell expansion in *Tg(hsp70:p210$^{BCR/ABL1}$)* fish was the result of increased proliferation (Figure 4A, B, E and F). However, myeloid cell apoptosis was also significantly decreased in *Tg(hsp70:p210$^{BCR/ABL1}$)* larvae and adult KM compared with WT controls, suggesting that the expansion of myeloid cells *Tg(hsp70:p210$^{BCR/ABL1}$)* was also caused by reduced apoptosis (Figure 4C, D, G and H).

### *Tg(hsp70:p210$^{BCR/ABL1}$)* transgenic cells with induced CML-like disease were transplantable

To determine the aggressiveness of the leukemia induced by *Tg(hsp70:p210$^{BCR/ABL1}$)* activity, whole KM blood cells from *Tg(hsp70:p210$^{BCR/ABL1}$)* fish were transplanted into γ-irradiated WT adult hosts and the resulting fish were tested to determine if the CML-like phenotype developed in the *Tg(hsp70:p210$^{BCR/ABL1}$)* fish could be transplanted into the WT fish. We used 1-year old *Tg(hsp70:p210$^{BCR/ABL1}$-lyz:DsRed)* CML-like donors and *Tg(lyz:DsRed)* control donors, in which the granulocytes were marked by red fluorescence. Each irradiated WT fish received 0.2 million KM blood cells from donors and were then raised under normal conditions. All four surviving recipients of *Tg(hsp70:p210$^{BCR/ABL1}$-lyz:DsRed)* CML-like donor cells developed CML-like disease within 2-3 weeks of transplantation with whole KM blood cells, indicated by infiltration of DsRed$^{+}$ granulocytes into the periphery (Figure 5A) and the robust expansion of myeloid cells in both the PB and KM (Figure 5B). In contrast, no control fish showed signs of a CML-like phenotype. We collected leukemia cells from the PB and KM and showed that these inflated cells were *BCR/ABL1*$^{+}$ by PCR (Figure 5C). We concluded that the myeloid cells that accumulated in *Tg(hsp70:p210$^{BCR/ABL1}$)* fish could proliferate autonomously and could cause CML-like disease in a WT host.

### *Tg(hsp70:p210$^{BCR/ABL1}$)* transgenic leukemic model responded to chemotherapeutic drug treatment

Recent studies demonstrated that zebrafish shares 82% of disease-associated targets and numerous drug metabolism pathways with humans.[12] To determine if the pharmacological mechanism in *Tg(hsp70:p210$^{BCR/ABL1}$)* transgenic zebrafish was also conserved compared with CML patients, we treated the WT and *Tg(hsp70:p210$^{BCR/ABL1}$)* embryos with the widely used anti-CML drugs, imatinib, dasatinib, and bosutinib, to the maximum teratogenic doses, with DMSO as a placebo (*Online Supplementary*

**Table 1.** Hemogram and classification of Tg(hsp70:p210BCR/ABL1) fish at 6-12 months

| Classification | Group | Number | Percentages in PB (%) | | | | Percentages in KM (%) | | | | Leukemia cell types |
|---|---|---|---|---|---|---|---|---|---|---|---|
| | | | Blasts | Myeloid precursors | Myelocytes | Lymphocytes | Blasts | Myeloid precursors | Myelocytes | Lymphocytes | |
| WT | Normal | 55 | 0.06 ± 0.04 | 1.68 ± 0.39 | 8.09 ± 1.45 | 90.17 ± 1.55 | 4.41 ± 0.56 | 12.56 ± 0.76 | 46.89 ± 1.29 | 36.14 ± 1.21 | |
| Tg(hsp70:p210BCR/ABL1) | CML-CP | 68 | 0.40 ± 0.12 | 2.99 ± 0.59 | 8.88 ± 1.24 | 87.73 ± 1.45 | 3.37 ± 0.51 | 12.16 ± 0.92 | 50.48 ± 1.39* | 34.00 ± 0.98 | Neutrophils and myeloid precursors |
| | CML-AP | 8 | 1.75 ± 0.82 | 19.00 ± 3.95† | 14.20 ± 3.06 | 65.05 ± 5.86 | 10.36 ± 1.32‡ | 18.54 ± 1.51† | 36.29 ± 2.98 | 34.82 ± 2.47 | Myeloid precursors and blasts |
| | CML-BP | 1 | 99.28§ | 0.26 | 0.13 | 0.33 | 90.25§ | 1.96 | 4.56 | 3.23 | Blasts |

The White blood cell counts were obtained by identifying at least 500 cells per kidney marrow (KM) preparation and at least 1500 cells per peripheral blood (PB) preparation. The percentages were indicated by mean ± SEM. Adult Tg(hsp70:p210BCR/ABL1) fish characterized by myelocytes > 15% in PB or > 50% in KM were divided into CML-CP, blasts usually account for < 2% in PB or < 5% in KM. Adult Tg(hsp70:p210BCR/ABL1) fish characterized by blasts > 10% in PB or KM were divided into CML-AP. Adult Tg(hsp70:p210BCR/ABL1) fish characterized by blasts > 90% in both PB and KM were divided into CML-BP. * Indicates myelocytes in PB or KM increased > 15% or 50%. † Indicates myeloid precursors in PB or KM increased > 10% or >15%. ‡ Indicates blasts in PB or KM increased > 10%. § Indicates blasts in PB or KM increased > 90%.

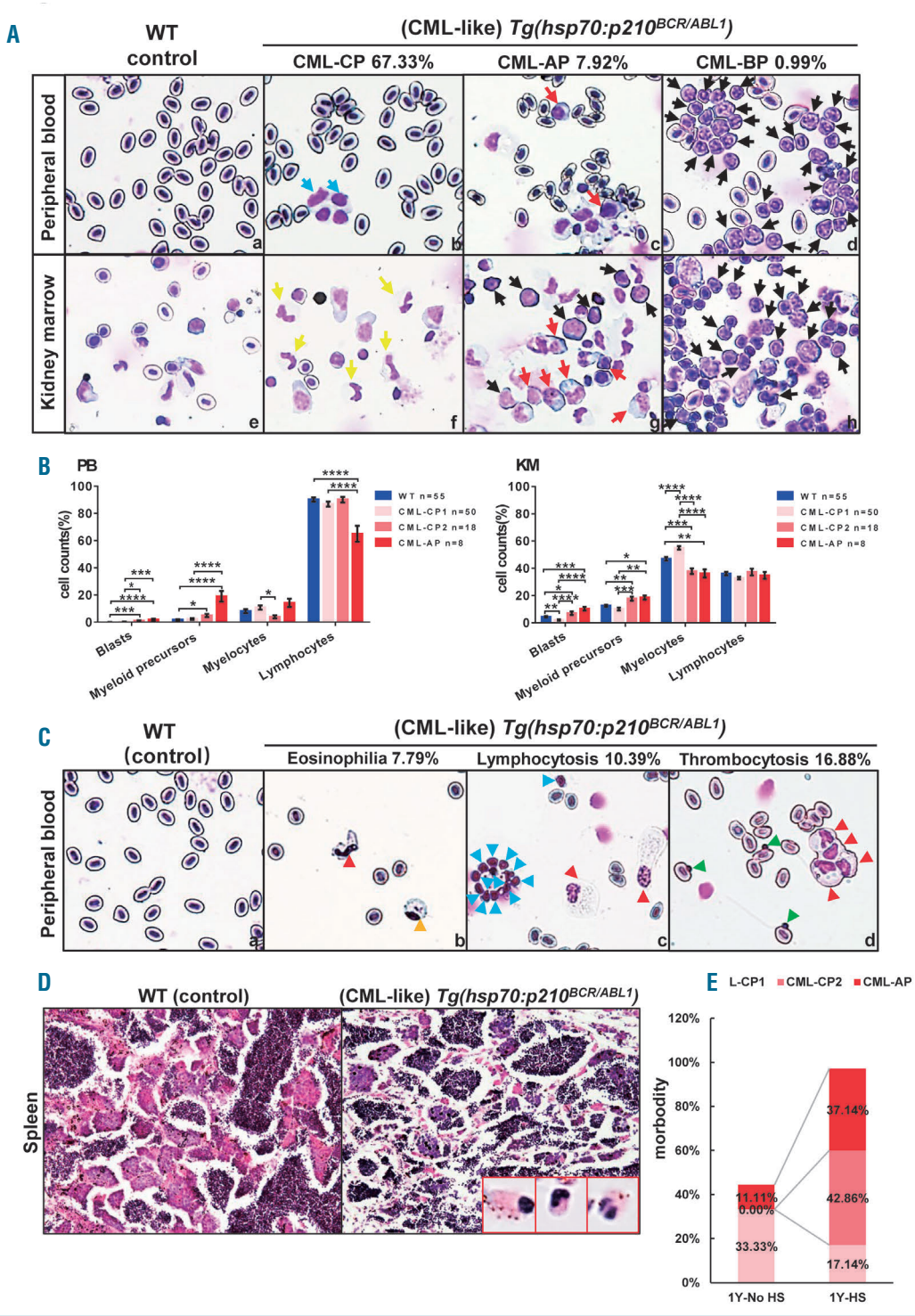


**Figure 3. *Tg(hsp70:p210$^{BCR/ABL1}$)* adult fish display abnormal myeloid cell expansion resembled chronic myeloid leukemia (CML)-like phenotypes.** (A) May-Grunwald-Giemsa staining of peripheral blood (PB) cells (top) and kidney marrow (KM) blood cells (bottom) were obtained from wild-type (WT) (a, e) (n=55) and *Tg(hsp70:p210$^{BCR/ABL1}$)* (b-d, f-h) (n=101) adult zebrafish. Blue arrows indicate accumulated promyelocytes in CML-chronic phase (CP)-like fish. Yellow arrows indicate neutrophils in CML-CP-like fish. Red arrows indicate myeloid precursors in CML accelerated phase (AP)-like fish. Black arrows indicate blasts in both CML-AP-like fish and CML-BP-like fish. The percentages indicate the ratio that number of fish with leukemia-like phenotype in total number of fish. Original magnification x400. (B) Statistical analysis. Blood cell counts of PB and KM were calculated manually based on their morphology. ANOVA; mean±Standard Error of Mean; *$P$<0.05; **$P$<0.01; ***$P$<0.001; ****$P$<0.0001. (C) Large numbers of eosinophils (b, yellow arrow), lymphocytes (c, blue arrow), and platelets (d, green arrow) accumulated in CML-like *Tg(hsp70:p210$^{BCR/ABL1}$)* adult fish PB compared with WT controls (a, n=55). The percentages indicate the ratio that number of fish with abnormal cells accumulated in total number of CML-like *Tg(hsp70:p210$^{BCR/ABL1}$)* adult fish. Red arrows indicate neutrophils. Original magnification x400. Stains were May-Grunwald-Giemsa. (D) Histology of the spleen from CML-like *Tg(hsp70:p210$^{BCR/ABL1}$)* adult fish showing disruption of the spleen architecture and massive invasion by hematopoietic cells compared with WT controls. Original magnifications x200 for each panel. Inset (red rectangles): granulocytic myeloid cells at higher magnification x1000. Stains were Hematoxylin & Eosin. (E) The morbidity rate of CML was higher in 1 Y-HS *Tg(hsp70:p210$^{BCR/ABL1}$)* adult fish (n=35) compared with 1 Y-No HS *Tg(hsp70:p210$^{BCR/ABL1}$)* adult fish (n=18), 97.14% and 44.44%, respectively. 1Y-No HS: 1-year-old *Tg(hsp70:p210$^{BCR/ABL1}$)* adult fish without heat shock treatment. 1Y-HS: 1-year-old *Tg(hsp70:p210$^{BCR/ABL1}$)* adult fish with heat shock treatment. The morbidity rates of *Tg(hsp70:p210$^{BCR/ABL1}$)* transgenic fish in the HS group developing into CML-CP 1 phase was 17.14%, while that in the No-HS treatment group was 33.33%. The morbidity rate of *Tg(hsp70:p210$^{BCR/ABL1}$)* transgenic fish in the heat shock treatment group developing into CML-CP 2 phase and CML-AP phase were 42.86% and 37.14%, compared with 0.00% and 11.11%, respectively, in the No-HS *Tg(hsp70:p210$^{BCR/ABL1}$)* adult fish.

*Figure S4*). After incubation with these TKI for 48 h, we calculated the numbers of *lcp1*$^{+}$ myeloid cells in WT and *Tg(hsp70:p210*$^{BCR/ABL1}$*)* larvae in the posterior blood island (PBI) region at 5 dpf (Figure 6A and B). All the TKI significantly reduced the number of *lcp1*$^{+}$ myeloid cells in *Tg(hsp70:p210*$^{BCR/ABL1}$*)* larvae compared with the DMSO control group. In addition, lower concentrations (20 and 40 μmol/L) of imatinib significantly reduced the expanded *lcp1*$^{+}$ myeloid population in *Tg(hsp70:p210*$^{BCR/ABL1}$*)* larvae, but the number of *lcp1*$^{+}$ myeloid cells was also significantly reduced in WT larvae at higher concentrations (80 μmol/L) compared with DMSO (*Online Supplementary Figure S5*). These results suggest that high doses of imatinib may affect normal myelopoiesis, which may be associated with more adverse events or unpredictable off-target effects. Further studies are needed to clarify these effects and to support the clinical treatment of patients with CML.

We screened a library of 171 compounds in 3 dpf WT and *Tg(hsp70:p210*$^{BCR/ABL1}$*)* embryos to examine their ability to reverse the disease phenotype. We reduced the incubation time to 24 h to speed up the screening process, and then calculated the numbers of *lcp1*$^{+}$ myeloid cells in WT and *Tg(hsp70:p210*$^{BCR/ABL1}$*)* larvae in the PBI region at 4 dpf. Ten inhibitors, including the natural compound, icaritin, as well as CC-223, BEZ235, AZD3759, icotinib, DB07268, NQDI-1, selonsertib (GS-4997), LY364947 and ciliobrevin A (HPI-4) effectively reduced the expanded *lcp1*$^{+}$ myeloid population in *Tg(hsp70:p210*$^{BCR/ABL1}$) embryos compared with DMSO-treated controls (Figure 6C).

## Discussion

We constructed a new germline of transgenic zebrafish expressing the hBCR/ABL1 fusion protein. Expression of hBCR/ABL1 in *Tg(hsp70:p210*$^{BCR/ABL1}$*)* transgenic zebrafish altered hematopoiesis by up-regulating myeloid genes, as detected in larvae at 3 dpf. Adult *Tg(hsp70:p210*$^{BCR/ABL1}$*)* transgenic zebrafish developed CML characterized by clonal myelocytic blasts, representing the first zebrafish model of hBCR/ABL1-induced CML. As the disease progressed, hematopoietic differentiation was interrupted, and immature blasts and myeloid precursors accumulated in the BM and spilled into the circulation in this zebrafish model, closely resembling the natural course of human CML progression without treatment. The most accurate CML animal model to date is the SCLtTA/BCR-ABL mouse line[21] established by Koschmieder *et al.* in 2005. However, these mice only survive for 4-17 weeks, while adult *Tg(hsp70:p210*$^{BCR/ABL1}$*)* transgenic zebrafish could survive for from 12 to >18 months, with or without heat shock, which was longer than all previous mouse models. The incidence of CML in the *Tg(hsp70:p210*$^{BCR/ABL1}$*)* transgenic model was increased by hBCR/ABL1 heat shock. This *Tg(hsp70:p210*$^{BCR/ABL1}$*)* transgenic model may thus provide insights into the mechanism that drives the transition from CML-CP to CML-AP or CML-BP.

Tyrosine kinase inhibitors (imatinib, dasatinib, and bosutinib) effectively reduced the expanded myeloid population in *Tg(hsp70:p210*$^{BCR/ABL1}$*)* embryos, suggesting that the pharmacological pathways in this model were similar to those in human CML. The discovery of imatinib has greatly improved the longevity and quality of life of patients with CML; however, some patients develop resistance to TKI and may even progress toward CML-AP or CML-BP of the disease despite TKI therapy. Second- and third-generation TKI were developed to treat patients in whom imatinib fails, with up to 40-87% of patients achieving durable complete cytogenetic remission.[4] However, more serious side-effects have recently been associated with these second- and third-generation TKI. Understanding the underlying cause of resistance and screening for novel targeted drugs with low toxicity and high efficiency thus remain important steps in combating CML. Further studies are planned to generate site-directed mutations of the ABL1 kinase domain in *Tg(hsp70:p210*$^{BCR/ABL1}$*)* transgenic zebrafish using gene-editing technology (such as CRISPR/Cas9). The ABL1 kinase domain is frequently mutated in clinical cases, and examination of these mutants may thus help to elucidate the mechanism responsible for TKI resistance.

In the present study, we screened a compound library and discovered 10 new targeted drugs that reduced the

**Table 2.** Hemogram and classification of *Tg(hsp70:p210*$^{BCR/ABL1}$*)* fish in chronic myeloid leukemia chronic phase.

| Classification | Group | Number | Percentages in PB (%) | | | | Percentages in KM (%) | | | | Location | Leukemia cell types |
|---|---|---|---|---|---|---|---|---|---|---|---|---|
| | | | Blasts | Myeloid precursors | Myelocytes | Lymphocytes | Blasts | Myeloid precursors | Myelocytes | Lymphocytes | | |
| Normal | | 55 | 0.06 ± 0.04 | 1.68 ± 0.39 | 8.09 ± 1.45 | 90.17 ± 1.55 | 4.41 ± 0.56 | 12.56 ± 0.76 | 46.89 ± 1.29 | 36.14 ± 1.21 | | |
| CML-CP 1 | I | 27 | 0.00 ± 0.00 | 1.29 ± 0.42 | 4.09 ± 1.16 | 94.62 ± 1.36 | 1.42 ± 0.42 | 8.15 ± 0.49 | 58.75 ± 0.90* | 31.68 ± 1.04 | KM | Neutrophils in various degrees of maturation |
| | II | 4 | 0.15 ± 0.15 | 3.27 ± 1.53 | 20.11 ± 7.08* | 76.46 ± 8.51 | 2.57 ± 0.93 | 10.68 ± 2.16 | 43.93 ± 3.51 | 42.82 ± 3.86 | PB | |
| | III | 19 | 0.38 ± 0.22 | 3.48 ± 1.52 | 17.79 ± 2.38* | 78.36 ± 2.63 | 2.79 ± 0.83 | 12.82 ± 2.38 | 52.06 ± 2.34* | 32.32 ± 1.59 | KM and PB | |
| CML-CP 2 | IV | 15 | 0.78 ± 0.31 | 3.40 ± 0.86 | 3.03 ± 0.67 | 92.79 ± 1.26 | 8.35 ± 1.24‡ | 19.07 ± 1.47† | 37.61 ± 2.36 | 34.98 ± 2.17 | KM | Myeloid precursors |
| | V | 3 | 2.45 ± 1.31‡ | 12.22 ± 3.83† | 8.26 ± 5.07 | 77.07 ± 7.69 | 0.71 ± 0.57 | 11.47 ± 4.02 | 39.07 ± 3.72 | 48.75 ± 8.09 | PB | |

White blood cell counts were obtained by identifying at least 500 cells per kidney marrow (KM) preparation and at least 1,500 cells per peripheral blood (PB) preparation. The percentages were indicated by mean±Standard Error of Mean. Chronic myeloid leukemia-chronic phase (CML-CP) 1: blasts <2%, myeloid precursors <10% in PB or blasts <5%, myeloid precursors <15% in KM. CML-CP 2: blasts >2%, myeloid precursors >10% in PB or blasts >5%, myeloid precursors >15% in KM. CML-CP 1-Group I: myelocytes increased in KM. CML-CP 1-Group II: myelocytes and myeloid precursors increased in PB. CML-CP 1-Group III: myelocytes increased in both PB and KM, myeloid precursors increased in PB. CML-CP 2-Group IV: myeloid precursors and blasts increased in KM. CML-CP 2-Group V: myeloid precursors and blasts increased in PB. *Indicates myelocytes in PB or KM increased by >15% or 50%. †Indicates myeloid precursors in PB or KM by >10% or >15%. ‡Indicates blasts in PB or KM increased by >2% or >5%.

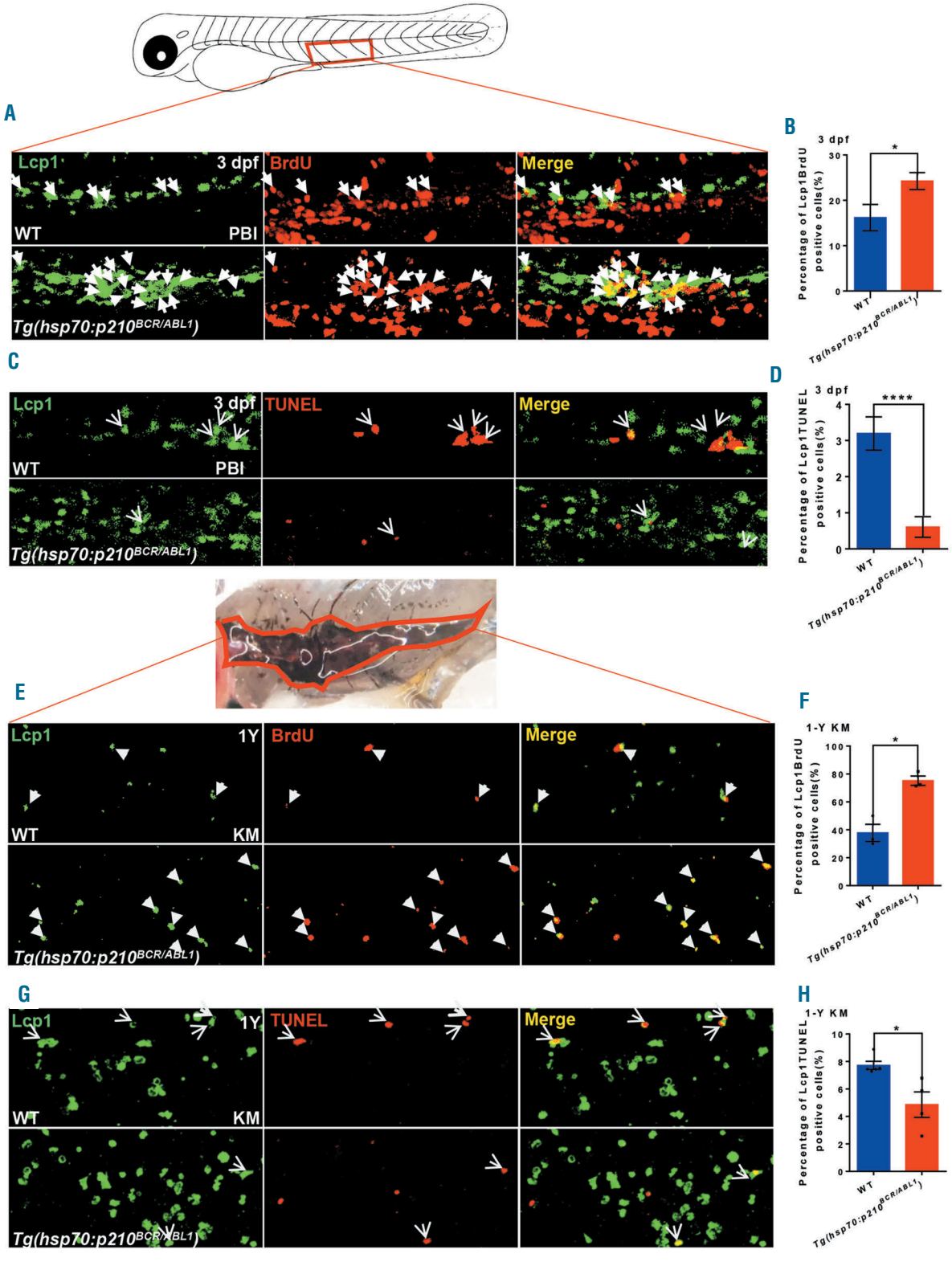


**Figure 4. The abnormal myeloid cell expansion in *Tg(hsp70:p210$^{BCR/ABL1}$)* fish caused by proliferation and apoptosis perturbation.** Lcp1 and BrdU antibody immunofluorescence double staining indicates a significant increase in the myeloid cells proliferation in the PBI region of 3 dpf HS *Tg(hsp70:p210$^{BCR/ABL1}$)* larvae (n=28) compared with the wild-type (WT) controls (n=18) (A and B) and kidney marrow (KM) Lcp1$^{+}$ cells in 1-year *Tg(hsp70:p210$^{BCR/ABL1}$)* adults (n=3) compared with the WT controls (n=3) (E and F). Lcp1 antibody and transferase dUTP nick end labeling (TUNEL) assay co-staining were used to detect the apoptosis. The number of Lcp1$^{+}$ cells in the PBI region (C and D)/KM (G and H) in 3 dpf/1-year HS *Tg(hsp70:p210$^{BCR/ABL1}$)* (n=27/n=4) significantly decreased compared with WT (n=19/n=5). Arrows indicate Lcp1BrdU/Lcp1TUNEL double-positive cells. Original magnification x100 (A, C, E, G). Percentage of the PBI region and KM localized Lcp1$^{+}$ myeloid cells that incorporate BrdU/TUNEL in Lcp1+ myeloid cells in 3 dpf or 1-year HS WT and *Tg(hsp70:p210$^{BCR/ABL1}$)* fish. Student *t*-test; mean±Standard Error of Mean; *$P$<0.05; ****$P$<0.0001.

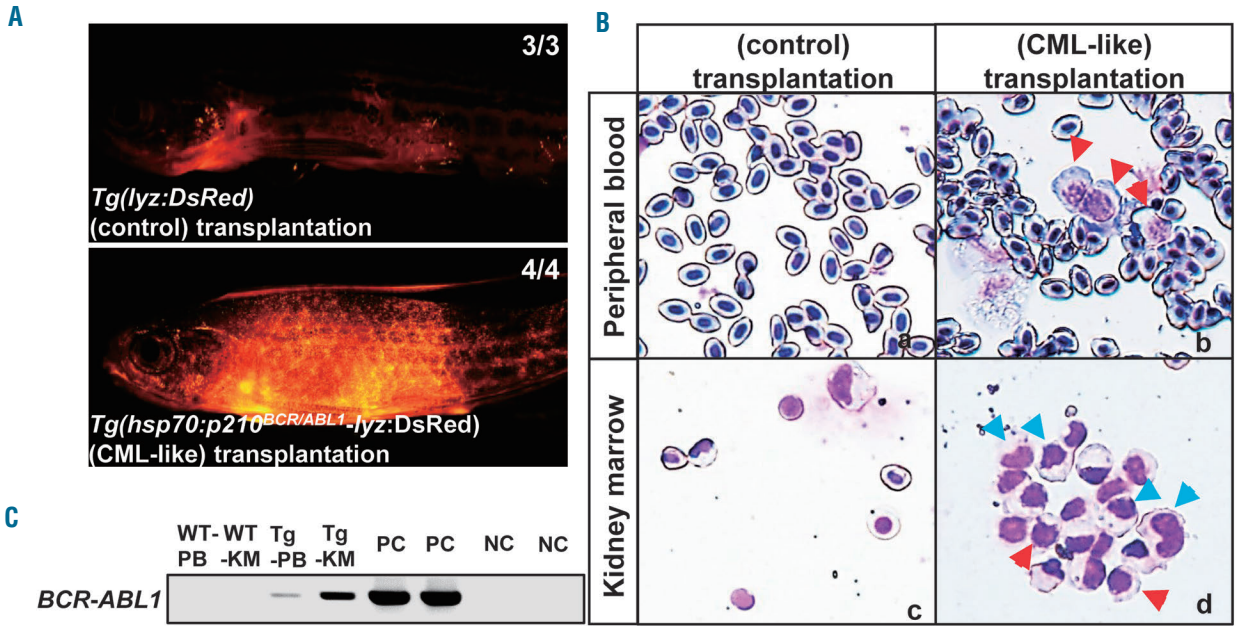


**Figure 5. Wild-type (WT) fish transplanted with chronic myeloid leukemia (CML)-like leukemic cells show myeloid expansion in the early stage.** Of 43 and 65 recipients transplanted with *Tg(lyz:DsRed)* control and CML-like *Tg(hsp70:p210$^{BCR/ABL1}$-lyz:DsRed)* kidney marrow (KM) cells, three and four survived, respectively. (A) DsRed positive cells repopulated in recipients within 2-3 weeks after transplantation of *Tg(lyz:DsRed)* control (left) and CML-like *Tg(hsp70:p210$^{BCR/ABL1}$-lyz:DsRed)* (right) KM blood cells. (B) All survived recipients were stained by May-Grunwald-Giemsa. Myelocytes (d, blue arrows) increased in KM of WT fish after transplanted with CML-like *Tg(hsp70:p210$^{BCR/ABL1}$-lyz:DsRed)* KM cells. Myeloid precursors (b and d, red arrows) increased in both peripheral blood (PB) and KM of WT fish after being transplanted with CML-like *Tg(hsp70:p210$^{BCR/ABL1}$-lyz:DsRed)* KM blood cells. Original magnification x400. (C) h*BCR/ABL1*$^{+}$ cDNA fragments detected in PB and KM cells of WT fish after being transplanted with *Tg(lyz:DsRed)* control (WT-PB/WT-KM) and CML-like *Tg(hsp70:p210$^{BCR/ABL1}$-lyz:DsRed)* KM cells (Tg-PB/Tg-KM) assessed by polymerase chain reaction. PC: pToL *hsp*70:p210$^{BCR/ABL1}$ as the positive control. NC: dd$H_2O$ as the negative control.

expanded myeloid population in *Tg(hsp70:p210$^{BCR/ABL1}$)* transgenic zebrafish embryos. Icaritin is a natural flavonoid derived from the traditional Chinese medicine Epimedium. Icaritin was previously shown to inhibit the growth of leukemic cell lines, including imatinib-resistant *BCR/ABL1*$^{+}$ blast cells and BCR/ABL1-T315I mutant cells *via* mechanisms involved in MAPK and JAK/STAT signaling.[27-29] The current results show that icaritin could reduce the expanded *lcp1*$^{+}$ myeloid population in *Tg(hsp70:p210$^{BCR/ABL1}$)* embryos, consistent with these previous findings. Overactivation of PI3K/AKT/mTOR is known to play a pivotal role in many human cancers, thus providing strong support for the therapeutic anticancer application of PI3K/Akt/mTOR inhibitors.[30,31] Sadovnik *et al.* found that escape of CML LSC was disrupted by the addition of PI3K/mTOR blockers.[32] Furthermore, the PI3K/mTOR dual inhibitor BEZ235 had beneficial effects on a variety of tumors *in vivo* and *in vitro*, including lymphoid malignancies[33] and myeloid malignancies.[34,35] Bendell also identified the active-site inhibitor CC-223, which targets both mTORC1 and mTORC2 through mTOR kinase activity to inhibit activation of AKT and 4EBP1, as a promising therapeutic agent with activity against many non-Hodgkin lymphoma and solid tumor cell lines.[36] In the current study, the *Tg(hsp70:p210$^{BCR/ABL1}$)* embryonic zebrafish model responded well to both BEZ235 and CC-223. Overall, these results suggest that targeting the PI3K/Akt/mTOR signaling pathway may be an effective strategy for overcoming CML therapy resistance. Unexpectedly, however, *Tg(hsp70:p210$^{BCR/ABL1}$)* larvae did not respond well to the sphingosine 1-phosphate antagonist, FTY720, and the number of *lcp1*$^{+}$ myeloid cells in WT zebrafish conversely increased after treatment with FTY720. Previous studies reported that the FTY720-mediated PP2A reactivation could markedly reduce the survival and self-renewal of CML-quiescent HSC through BCR-ABL1 kinase-independent and PP2A-mediated inhibition of JAK2 and β-catenin.[37] We therefore hypothesized that, although sphingosine 1-phosphate may play a role in hematopoietic regulation, further studies are needed to determine its precise mechanism. LY364947,[38,39] ciliobrevin A,[40] DB07268,[41] selonsertib,[42] NQDI-1,[43] AZD3759,[44] and icotinib[45] have recently been shown to target key factors and signaling pathways essential for the survival of CML LSC and other CSC, including transforming growth factor β,[39] Hedgehog,[46] c-Jun N-terminal kinases,[47] apoptosis signal-regulating kinase 1,[48] and epidermal growth factor receptor.[49] The *Tg(hsp70:p210$^{BCR/ABL1}$)* transgenic zebrafish embryos in the current study also responded well to these compounds. Our findings, therefore, suggest that inhibition of BCR/ABL1 kinase-dependent or kinase-independent pathways (Figure 6D) might offer potential for overcoming resistance to TKI and thus eradicate LSC, thereby paving the way for the development of novel, more effective LSC-eradicating treatment strategies for CML.

In conclusion, the *Tg(hsp70:p210$^{BCR/ABL1}$)* transgenic model represents a phenotype-based, cost-effective, *in vivo* model of CML suitable for high-throughput chemical screening. This model may improve our understanding of

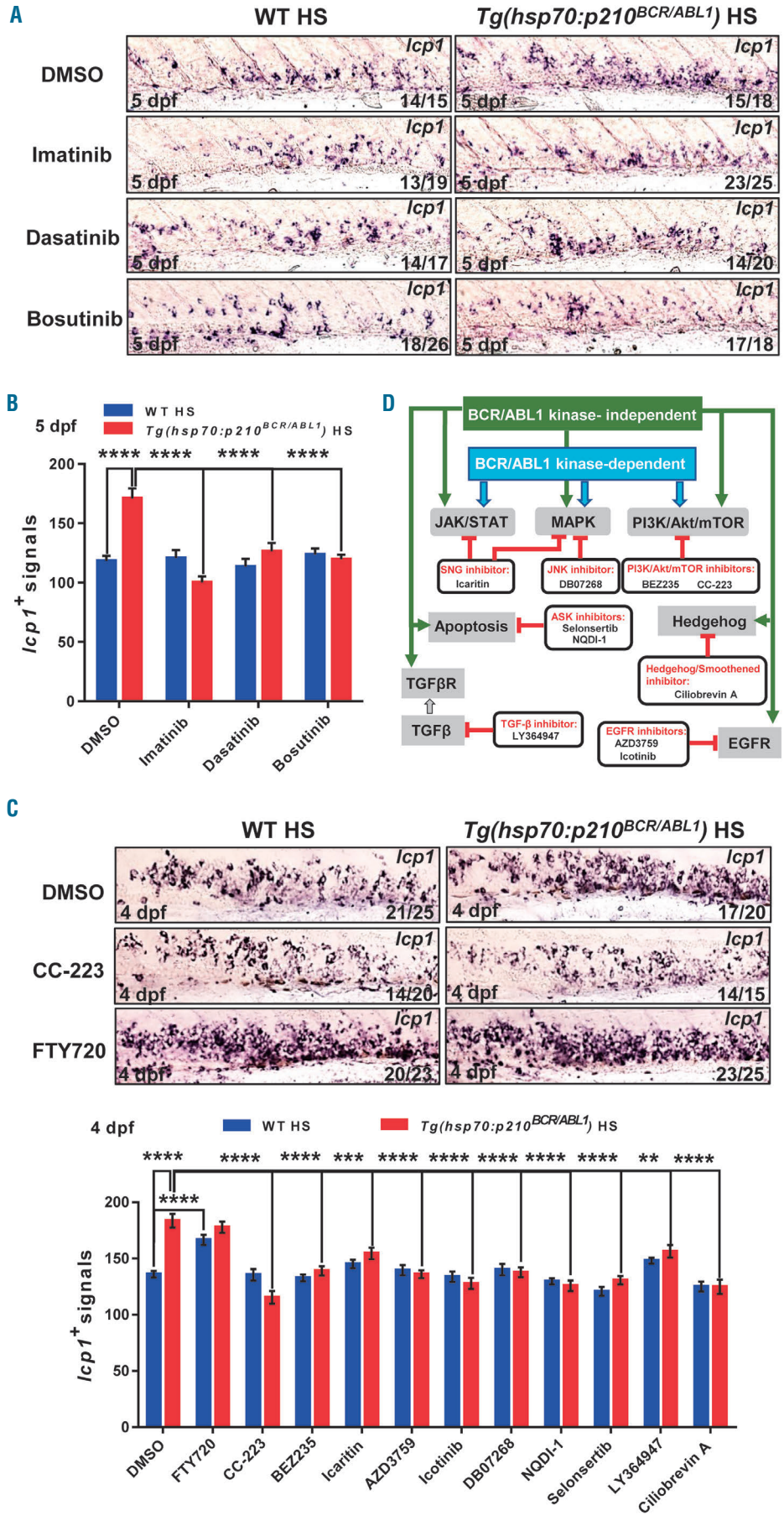


**Figure 6. *Tg(hsp70:p210$^{BCR/ABL1}$)* transgenic zebrafish model responds to chemotherapy.** (A and B) TKI treatment in zebrafish larvae. 3 dpf HS WT (left panels) and *Tg(hsp70:p210$^{BCR/ABL1}$)* (right panels) larvae treated for 48 hours with 1‰ DMSO control, 20 μmol/L imatinib, 5 μmol/L dasatinib and 10 μmol/L bosutinib. (A) WISH of *lcp1* expression in the drug treated larvae at 5 dpf. n/n, number of zebrafish larvae showing representative phenotype/total number of zebrafish larvae examined. Original magnification, x200. (Bottom): statistical analysis. Enumeration of *lcp1*$^+$ signals shown in (A). Average numbers of *lcp1*$^+$ cells per larva with drug treatment. ANOVA; mean ± SEM; ****$P$<0.0001. (C) Drug screening. Upper: WISH of *lcp1* expression in *Tg(hsp70:p210$^{BCR/ABL1}$)* (right) larvae and WT controls (left) at 4 dpf after treatment (1‰ DMSO, 20 μmol/L CC-223, 2.5 μmol/L FTY720) for 24 hours. n/n, number of zebrafish larvae showing representative phenotype/total number of zebrafish larvae examined. Original magnification, x200. Under: Statistical analysis. 3 dpf HS WT and *Tg(hsp70:p210$^{BCR/ABL1}$)* larvae (n=25 and n=20, n=23 and n=25, n=20 and n=15, n=22 and n=24, n=20 and n=21, n=14 and n=24, n=19 and n=19, n=20 and n=19, n=19 and n=18, n=23 and n=24, n=23 and n=17, n=16 and n=15, respectively) were treated for 24 hours with drugs (1‰ DMSO, 2.5 μmol/L FTY720, 20 μmol/L CC-223, 0.5 μmol/L BEZ235, 40 μmol/L icaritin, 20 μmol/L AZD3759, 80 μmol/L icotinib, 40 μmol/L DB07268, 80 μmol/L NQDI-1, 40 μmol/L selonsertib, 20 μmol/L LY364947, 1 μmol/L ciliobrevin A, respectively). Average numbers of *lcp1*$^+$ cells per larva with drug treatment. ANOVA; mean ± SEM; **$P$<0.01; ***$P$<0.001; ****$P$<0.0001. (D) Sketch map of inhibitors target BCR/ABL1 kinase-dependent or kinase-independent pathways. JNK: the c-Jun N-terminal kinase. ASK: apoptosis signal-regulating kinase. TGF-β, the transforming growth factor β. EGFR: the epidermal growth factor receptor.

the protein functions, pharmacological mechanisms, and toxicology of novel targeted drugs, thus improving the cure rate for patients with CML.

***Acknowledgments***

*The authors would like to thank Dr. Nathan Lawson and Dr. Koichi Kawakami for providing pTol vector. The authors would like to thank Dr. Zilong Wen for providing Lcp1 antibody. The authors would like to thank Dr. Kuangyu Yen, Dr. Yali Chi, Dr. Shan Xiao, Xiaohui Chen, and Yi Zheng for their helpful suggestion. The authors would like to thank Christine Walsh, Hank Duan and the editor of International Science Editing for correcting the grammar and spelling. This work was supported by the Young Teacher National Natural Science Foundation of China (Grant No. 81700150), the Natural Science Foundation of Guangdong Province, China (Grant No. 2014A030312002), the Department of Science and Technology of Guangdong Province, China (Grant No. 2015B050501006) and Shunde Economy, Science and Technology Bureau, China (Grant No. 2015CXTD06).*

## References

1. von Bubnoff N, Pleyer L, Neureiter D, Faber V, Duyster J. Chronic myelogenous leukemia (CML). In: Greil R, Pleyer L, Faber V, Neureiter D, eds. Chronic Myeloid Neoplasias and Clonal Overlap Syndromes: Epidemiology, Pathophysiology and Treatment Options. Vienna: Springer Vienna, 2010:117-152.
2. Champlin RE, Golde DW. Chronic myelogenous leukemia: recent advances. Blood. 1985;65(5):1039-1047.
3. Cotta CV, Bueso-Ramos CE. New insights into the pathobiology and treatment of chronic myelogenous leukemia. Ann Diag Pathol. 2007;11(1):68-78.
4. Apperley JF. Chronic myeloid leukaemia. Lancet. 2015;385(9976):1447-1459.
5. Rowley JD. Letter: A new consistent chromosomal abnormality in chronic myelogenous leukaemia identified by quinacrine fluorescence and Giemsa staining. Nature. 1973;243(5405):290-293.
6. Melo JV. The diversity of BCR-ABL fusion proteins and their relationship to leukemia phenotype. Blood. 1996;88(7):2375-2384.
7. Shtivelman E, Lifshitz B, Gale RP, Roe BA, Canaani E. Alternative splicing of RNAs transcribed from the human abl gene and from the bcr-abl fused gene. Cell. 1986; 47(2):277-284.
8. Ben-Neriah Y, Daley GQ, Mes-Masson AM, Witte ON, Baltimore D. The chronic myelogenous leukemia-specific P210 protein is the product of the bcr/abl hybrid gene. Science. 1986;233(4760):212-214.
9. Ren R. Mechanisms of BCR-ABL in the pathogenesis of chronic myelogenous leukaemia. Nat Rev Cancer. 2005;5(3):172-183.
10. An X, Tiwari AK, Sun Y, Ding P-R, Ashby CR, Jr., Chen Z-S. BCR-ABL tyrosine kinase inhibitors in the treatment of Philadelphia chromosome positive chronic myeloid leukemia: A review. Leuk Res. 2010;34(10):1255-1268.
11. Ross TS, Mgbemena VE. Re-evaluating the role of BCR/ABL in chronic myelogenous leukemia. Mol Cell Oncol. 2014;1(3): e963450-e963450.
12. MacRae CA, Peterson RT. Zebrafish as tools for drug discovery. Nat Rev Drug Discov. 2015;14(10):721-731.
13. Westerfield M. The Zebrafish Book. A Guide for the Laboratory Use of Zebrafish (Danio rerio). University of Oregon Press, Eugene., 2000.
14. Kimmel CB, Ballard WW, Kimmel SR, Ullmann B, Schilling TF. Stages of embryonic development of the zebrafish. Dev Dyn. 1995;203(3):253-310.
15. Hall C, Flores MV, Storm T, Crosier K, Crosier P. The zebrafish lysozyme C promoter drives myeloid-specific expression in transgenic fish. Bmc Dev Biol. 2007;7:42.
16. He YP, Wertheim JA, Xu LW, et al. The coiled-coil domain and Tyr177 of bcr are required to induce a murine chronic myelogenous leukemia-like disease by bcr/abl. Blood. 2002;99(8):2957-2968.
17. Jin H, Sood R, Xu J, et al. Definitive hematopoietic stem/progenitor cells manifest distinct differentiation output in the zebrafish VDA and PBI. Development. 2009;136(4):647-654.
18. Adam A, Bartfai R, Lele Z, Krone PH, Orban L. Heat-inducible expression of a reporter gene detected by transient assay in zebrafish. Exp Cell Res. 2000;256(1):282-290.
19. Halloran MC, Sato-Maeda M, Warren JT, et al. Laser-induced gene expression in specific cells of transgenic zebrafish. Development. 2000;127(9):1953-1960.
20. Roumiantsev S, de Aos IE, Varticovski L, Ilaria RL, Van Etten RA. The Src homology 2 domain of Bcr/Abl is required for efficient induction of chronic myeloid leukemia-like disease in mice but not for lymphoid leukemogenesis or activation of phosphatidylinositol 3-kinase. Blood. 2001;97(1):4-13.
21. Koschmieder S, Gottgens B, Zhang P, et al. Inducible chronic phase of myeloid leukemia with expansion of hematopoietic stem cells in a transgenic model of BCR-ABL leukemogenesis. Blood. 2005; 105(1):324-334.
22. Honda H, Oda H, Suzuki T, et al. Development of acute lymphoblastic leukemia and myeloproliferative disorder in transgenic mice expressing p210(bcr/abl): A novel transgenic model for human Ph-1-positive leukemias. Blood. 1998;91(6):2067-2075.
23. Huettner CS, Koschmieder S, Iwasaki H, et al. Inducible expression of BCR/ABL using human CD34 regulatory elements results in a megakaryocytic myeloproliferative syndrome. Blood. 2003;102(9):3363-3370.
24. Sabattini E, Bacci F, Sagramoso C, Pileri SA. WHO classification of tumours of haematopoietic and lymphoid tissues in 2008: an overview. Pathologica. 2010;102(3):83-87.
25. Dowding C, Th'ng KH, Goldman JM, Galton DA. Increased T-lymphocyte numbers in chronic granulocytic leukemia before treatment. Exp Hematol. 1984;12(10):811-815.
26. Mason JE Jr, DeVita VT, Canellos GP. Thrombocytosis in chronic granulocytic leukemia: incidence and clinical significance. Blood. 1974;44(4):483-487.
27. Zhu JF, Li ZJ, sen Zhang G, et al. Icaritin Shows Potent Anti-Leukemia Activity on Chronic Myeloid Leukemia In Vitro and In Vivo by Regulating MAPK/ERK/JNK and JAK2/STAT3/AKT Signalings. Plos One. 2011;6(8): e23720.
28. Zhu S, Wang Z, Li Z, et al. Icaritin suppresses multiple myeloma, by inhibiting IL-6/JAK2/STAT3. Oncotarget. 2015;6(12):10460-10472.
29. Chen M, Turhan AG, Ding H, Lin Q, Meng K, Jiang X. Targeting BCR-ABL(+) stem/progenitor cells and BCR-ABL-T315I mutant cells by effective inhibition of the BCR-ABL-Tyr177-GRB2 complex. Oncotarget. 2017;8(27):43662-43677.
30. Xia P, Xu X-Y. PI3K/Akt/mTOR signaling pathway in cancer stem cells: from basic research to clinical application. Am J Cancer Res. 2015;5(5):1602-1609.
31. Polivka J Jr, Janku F. Molecular targets for cancer therapy in the PI3K/AKT/mTOR pathway. Pharmacol Ther. 2014;142(2):164-175.
32. Sadovnik I, Hoelbl-Kovacic A, Herrmann H, et al. Identification of CD25 as STAT5-Dependent Growth Regulator of Leukemic Stem Cells in Ph+ CML. Clin Cancer Res. 2016;22(8):2051-2061.
33. Wong J, Welschinger R, Hewson J, Bradstock KF, Bendall LJ. Efficacy of dual PI-3K and mTOR inhibitors in Vitro and in Vivo in acute lymphoblastic leukemia. Oncotarget. 2014;5(21):10460-10472.
34. Deng L, Jiang L, Lin X-H, et al. The PI3K/mTOR dual inhibitor BEZ235 suppresses proliferation and migration and reverses multidrug resistance in acute myeloid leukemia. Acta Pharmacol Sin. 2017;38(3):382-391.
35. Xin P, Li C, Zheng Y, et al. Efficacy of the dual PI3K and mTOR inhibitor NVP-BEZ235 in combination with imatinib mesylate against chronic myelogenous leukemia cell lines. Drug Des Deve Ther. 2017;11:1115-1126.
36. Bendell JC, Kelley RK, Shih KC, et al. A Phase I dose-escalation study to assess safety, tolerability, pharmacokinetics, and preliminary efficacy of the dual mTORC1/mTORC2 kinase inhibitor CC-223 in patients with advanced solid tumors or multiple myeloma. Cancer. 2015; 121(19):3481-3490.
37. Neviani P, Harb JG, Oaks JJ, et al. PP2A-activating drugs selectively eradicate TKI-resistant chronic myeloid leukemic stem cells. J Clin Invest. 2013;123(10):4144-4157.
38. Pellicano F, Holyoake TL. Assembling defenses against therapy-resistant leukemic stem cells: Bcl6 joins the ranks. J Exp Med. 2011;208(11):2155-2158.

39. Naka K, Hoshii T, Muraguchi T, et al. TGF-beta-FOXO signalling maintains leukaemia-initiating cells in chronic myeloid leukaemia. Nature. 2010; 463(7281):676-680.
40. Xiang W, Jiang T, Guo F, et al. Hedgehog pathway inhibitor-4 suppresses malignant properties of chondrosarcoma cells by disturbing tumor ciliogenesis. Oncol Rep. 2014;32(4):1622-1630.
41. Liu M, Wang S, Clampit JE, et al. Discovery of a new class of 4-anilinopyrimidines as potent c-Jun N-terminal kinase inhibitors: Synthesis and SAR studies. Bioorg Med Chem Lett. 2007;17(3):668-672.
42. Lin JH, Zhang JJ, Lin S-L, Chertow GM. Design of a Phase 2 Clinical trial of an ASK1 inhibitor, GS-4997, in patients with diabetic kidney disease. Nephron. 2015; 129(1):29-33.
43. Volynets GP, Chekanov MO, Synyugin AR, et al. Identification of 3H-Naphtho 1,2,3-de quinoline-2,7-diones as inhibitors of apoptosis signal-regulating kinase 1 (ASK1). J Med Chem. 2011;54(8):2680-2686.
44. Zeng Q, Wang J, Cheng Z, et al. Discovery and evaluation of clinical candidate AZD3759, a potent, oral active, central nervous system-penetrant, epidermal growth factor receptor tyrosine kinase Inhibitor. J Med Chem. 2015;58(20):8200-8215.
45. Tan F, Shen X, Wang D, et al. Icotinib (BPI-2009H), a novel EGFR tyrosine kinase inhibitor, displays potent efficacy in preclinical studies. Lung Cancer. 2012; 76(2):177-182.
46. Hyman JM, Firestone AJ, Heine VM, et al. Small-molecule inhibitors reveal multiple strategies for Hedgehog pathway blockade. Proc Natl Acad Sci U S A. 2009; 106(33): 14132-14137.
47. Redig AJ, Vakana E, Platanias LC. Regulation of mammalian target of rapamycin and mitogen activated protein kinase pathways by BCR-ABL. Leuk Lymphoma. 2011;52 suppl 1:45-53.
48. Bellazzo A, Di Minin G, Collavin L. Block one, unleash a hundred. Mechanisms of DAB2IP inactivation in cancer. Cell Death Differ. 2017;24(1):15-25.
49. Corrado C, Saieva L, Raimondo S, Santoro A, De Leo G, Alessandro R. Chronic myelogenous leukaemia exosomes modulate bone marrow microenvironment through activation of epidermal growth factor receptor. J Cell Mol Med. 2016;20(10): 1829-1839.